Generalized Cutler-Mott relation in a crossover between Fermi and non-Fermi liquid regimes of two-site charge Kondo simulators

T. K. T. Nguyen [1,*] and M. N. Kiselev [2]

[1] *Institute of Physics, Vietnam Academy of Science and Technology, 10 Dao Tan, 118000 Hanoi, Vietnam*

[2] *The Abdus Salam International Centre for Theoretical Physics, Strada Costiera 11, I-34151, Trieste, Italy*

(Received 18 August 2025; revised 5 February 2026; accepted 11 February 2026; published 18 March 2026)

We analyze the validity of the Cutler-Mott relations outside the Landau Fermi-liquid concept. We consider a two-site charge Kondo circuit as a paradigmatic example of a system possessing both Fermi- and non-Fermi-liquid properties. It is shown that the generalized Cutler-Mott-like relations derived in the paper hold in both operating regimes of the charge Kondo quantum circuit, describing a smooth crossover between low- and high-temperature regimes. We discuss the applicability of the generalized Cutler-Mott relations for computing a figure of merit for the non-Fermi-liquid quantum simulators.

DOI: 10.1103/5t1p-l36f

I. INTRODUCTION

Thermoelectricity, which describes the direct conversion between heat and electrical energy, has attracted considerable attention in recent years from both physicists and engineers. The study of thermoelectric effects provides valuable insight into the electronic structure and fundamental scattering processes within a system. Furthermore, thermoelectric materials can be utilized to generate electricity, measure temperature, or alter the temperature of objects through the reversible effects of Seebeck, Peltier, and Thomson [1].

The Seebeck effect [2] occurs when a temperature gradient is applied across two dissimilar electrical conductors or semiconductors, resulting in a voltage difference between them [3,4]. The efficiency of this conversion of thermoelectric energy is characterized by the Seebeck coefficient, or thermopower (TP), which is defined as the ratio of the generated electric voltage V_{th} to the temperature difference ΔT: $S = -eV_{th}/\Delta T$. The measurement of the thermovoltage V_{th} offers independent information about the thermoelectric coefficient G_T. The temperature difference ΔT is regulated using a current-heating technique. The differential electrical conductance G is measured using a variable external energy source. In the linear regime, TP is typically determined by the relation $S = G_T/G$. TP is a fundamental property that defines the thermoelectric performance of a material, making its enhancement both crucial and challenging. With advances in nanotechnology, numerous nanostructured devices have demonstrated promising improvements in TP.

It is well established that the TP is a valuable probe of Kondo correlations [5]. Thermodynamically, it is consistent with the entropy associated with the flow of charge in a material. In typical metals and degenerate semiconductors, only a fixed population of electrons, those with energies close to the Fermi energy within a few temperatures, contribute to both charge and thermoelectric transport. As the temperature decreases, the narrowing of the Fermi-Dirac distribution leads to a linear reduction in the Seebeck coefficient. Under the rigid-band approximation, the Cutler-Mott (CM) formula is commonly used to interpret the TP.

The CM relation, introduced by Cutler and Mott in 1969 [6], connects the TP to the energy derivative of the electrical conductance near the Fermi level as

$$S = \frac{\pi^2}{3}\frac{k_B^2 T}{e}\left[\frac{d\ln[G(E)]}{dE}\right]_{E=E_F}, \tag{1}$$

providing deep insight into the electronic structure and scattering mechanisms of a material. It has become a cornerstone in the study of thermoelectric properties, particularly in the context of metallic and metallic-like materials, where it describes the temperature dependence of the TP.

As shown in Eq. (1), the CM relation exhibits several notable properties [7]. First, the formula includes a term $k_B/e \sim 80\ \mu$V/K, which can be regarded as the natural unit of TP. Second, the derivative of the logarithm of conductivity in the expression highlights that TP is a highly sensitive probe of the electronic structure of the material. Third, the observed linear temperature dependence suggests that this behavior is characteristic of metallic and metal-like materials. Finally, the CM formula encodes information about scattering processes within the material.

While the CM relation has been remarkably successful in characterizing metallic systems and weakly interacting QDs, it breaks down in the presence of strong electronic correlations, such as those encountered in Coulomb-blockaded devices [8] or Kondo correlated nanostructures [9]. In Ref. [8], Turek and Matveev investigate the TP of single-electron transistors in the cotunneling regime, where charge transport proceeds via virtual intermediate states rather than through sequential tunneling. Their analysis applies in the low-temperature cotunneling regime ($T \ll E_C$, with $E_C = e^2/2C$ the QD charging energy), where elastic and inelastic

*Contact author: nkthanh@iop.vast.vn

cotunneling dominate conduction and the TP exhibits only a weak temperature dependence. In this strongly interacting regime, the CM relation is no longer valid and must be replaced by explicit microscopic calculations. Consistent with this, studies have demonstrated that deviations from the CM law in thermoelectric transport through QDs in the conventional spin Kondo regime originate from strong interactions between localized spins and conduction electrons [10].

The charge Kondo effect, in contrast to the conventional spin Kondo effect [11], arises from the twofold degeneracy of the charge degree of freedom at a Coulomb peak. Here, the N and $N+1$ charge states play the role of a spin-1/2 impurity, allowing the QD to be modeled as an effective isospin-1/2 magnetic impurity. This mechanism, first formulated by Flensberg, Matveev, and Furusaki [12–14], is realized in large metallic QDs strongly coupled to leads via nearly transparent quantum point contacts (QPCs). Electrons inside and outside the dot correspond to isospin-up and isospin-down states, respectively, and backscattering at the QPC flips the isospin as electrons tunnel in and out. Additional internal degrees of freedom—such as electron spin [9,15,16] or the number of single-mode QPCs [17,18]—set the number of effective Kondo channels.

A comprehensive analysis of TP oscillations in the charge Kondo regime was carried out by Andreev and Matveev [9], who studied a large metallic QD weakly coupled to one lead and strongly coupled to another via an almost transparent QPC. They demonstrated that, in such systems, the standard CM relation breaks down because of the emergence of Kondo correlations. Although the TP retains an oscillatory dependence on the gate voltage, neither its amplitude nor its sign is captured by the conventional CM law; instead, explicit microscopic expressions are required. In the two-channel charge Kondo model, the system enters a non-Fermi-liquid (NFL) regime at intermediate temperatures ($\Gamma \ll T \ll T_K$), where the Kondo temperature is set by the QD charging energy ($T_K \sim E_C$) and the Kondo resonance width scales as $\Gamma \sim |r|^2 E_C$, with $|r|$ denoting the Kondo interaction parameter. At sufficiently low temperatures ($T \ll \Gamma$), the system crosses over to a Fermi-liquid (FL) regime [9,15]. Moreover, the application of an arbitrarily small magnetic field drives a crossover from the NFL fixed point of the two-channel Kondo (2CK) model to the FL fixed point of the single-channel Kondo (1CK) model [19]. In the FL regime, the CM relation is restored [9,15,19,20]. Conversely, deviations from CM behavior induced by a finite in-plane magnetic field within the FL regime may serve as an indicator of the onset of NFL physics [19,21].

These results naturally raise a central question: Can the CM relation be generalized to charge Kondo systems operating in the NFL regime? A positive answer would provide a powerful and experimentally accessible method for probing TP in strongly correlated charge Kondo devices.

Building on a comparison between the traditional CM prediction and the nonperturbative results of Ref. [22], we introduce a generalized Cutler-Mott (GCM) relation for a two-site charge Kondo circuit (2SCKC). We demonstrate that this GCM relation accurately describes both FL and NFL regimes and can be extended to a broad class of charge Kondo systems. In addition, we show that the GCM framework provides a useful tool for analyzing thermoelectric performance, including the figure of merit.

The paper is structured as follows. In Sec. II, we introduce the theoretical model and review the standard CM relation in the context of the 2SCKC. Section III presents our proposed GCM relation and discusses its physical implications. In Sec. IV, we explore the extension of GCM to other charge Kondo systems. Section V focuses on the application of GCM to the figure of merit. Finally, we summarize our findings and conclusions in Sec. VI.

II. MODEL AND CUTLER-MOTT RELATION OF A TWO-SITE CHARGE KONDO CIRCUIT

In this paper, we examine the validity of the CM formula in a 2SCKC. The model, illustrated in Fig. 1(a), was theoretically proposed in Ref. [23] and has recently been experimentally implemented [24]. Each charge Kondo circuit (CKC) consists of a QD-QPC structure. The two CKCs are weakly coupled via a central QPC that connects the two QDs. This central QPC can be tuned into a nearly fully reflecting regime. We assume that the QPC is sufficiently long such that the charge quantization in each QD remains unaffected by any capacitive coupling between them. The QD is a large metallic island (depicted in dark red and blue cross-hatched areas, surrounded by black lines) that is electronically connected to a two-dimensional electron gas (2DEG, represented by the orange and grey continuous areas). The 2DEG is coupled to two large electrodes via two QPCs. Under a strong magnetic field applied perpendicular to the 2DEG plane, the system is tuned into the integer quantum Hall (IQH) regime at filling factor $\nu = 1$. The QPCs are adjusted to be nearly transparent, so that the chiral edge currents (red solid lines with arrows) experience only weak backscattering. CKCs operated in the IQH regime have been realized in breakthrough experiments [17,18]. Because the number of Kondo channels is set by the number of QPCs connected to the metallic QD, these devices offer direct experimental access to multichannel Kondo (MCK) physics. A defining feature of an MCK configuration is the emergence of NFL behavior [25–27], associated with an underlying $\mathbb{Z}_M$ symmetry.

In this work, we investigate a configuration in which the reflection amplitudes are identical at both QPCs in each CKC: $|r_{11}| = |r_{12}| = |r_1|$ and $|r_{21}| = |r_{22}| = |r_2|$, representing the 2CK setup of each CKC. The tunneling current through the central weak link can be determined by applying Kirchhoff's laws to the equivalent electrical circuit. To generate a thermoelectric response, the left CKC is maintained at a higher temperature, $T + \Delta T$, while the right CKC is kept at temperature T. This temperature gradient induces a thermal bias across the central weak link.

The equivalent circuit of the device is shown in Fig. 1(b). The $C_{\alpha,j}, R_{\alpha,j}$ ($\alpha, j = 11, 12, 21, 22$) and C_I, R_I characterize the QPCs and the weak central coupling, respectively. Additionally, we include the capacitors C_{g1}, C_{g2} and the gate voltages for the QDs, which are not shown in Fig. 1(a). The resistors R_1, R_2, and R_3 are used to divide the input gate voltage V_g. Consequently, the dimensionless gate voltages of

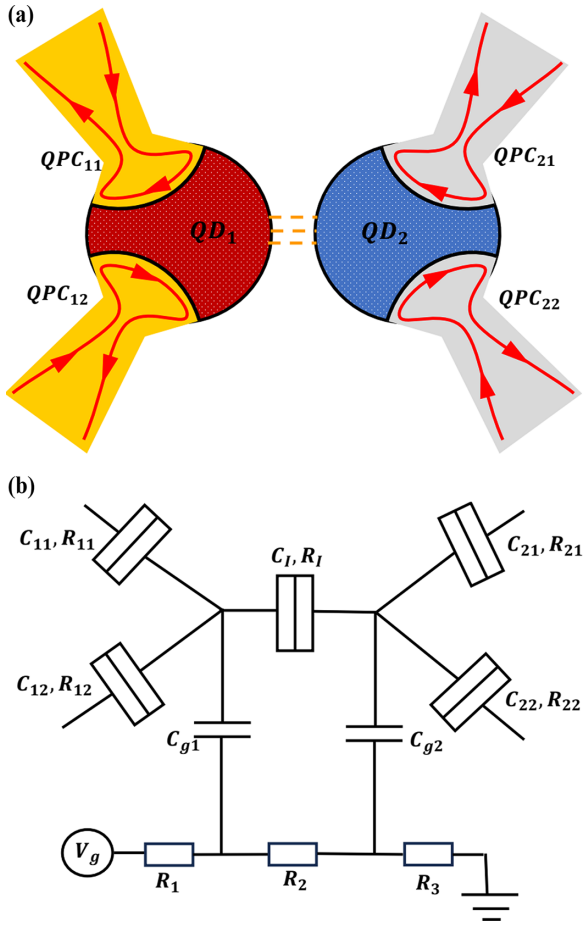

FIG. 1. (a) Schematic of a weak link between two charge Kondo circuits (CKCs). Each circuit consists of a large metallic island (QD), which is embedded into two-dimensional electron gas (2DEG) and connected to two large electrodes through single-mode quantum point contacts (QPCs). The 2DEG (plain area) is in the integer quantum Hall regime $\nu = 1$. The red line with arrows denotes the chiral edge mode that backscatters at the center of the narrow constriction. The QPCs are finely tuned to different regimes. The right CKC (gray color) is at the reference temperature T while the left circuit (orange color) is at a higher temperature $T + \Delta T$. (b) The equivalent circuit where the capacitors C_{g1}, C_{g2} and the componenents supporting the gate voltages for the QDs are not shown in (a). The resistors R_1, R_2, and R_3 are used to divide the input gate voltage V_g.

the QDs are estimated as follows:

$$N_1 = \frac{C_{g1}}{e}\frac{R_2+R_3}{R_t}V_g, \quad N_2 = \frac{C_{g2}}{e}\frac{R_3}{R_t}V_g, \tag{2}$$

with $R_t = R_1 + R_2 + R_3$. In fact, the resistors are variable. We find that if $C_{g1} = C_{g2}$ we can have $N_1 = N_2$ if $R_2 = 0$ or $N_2 = 0$ if $R_3 = 0$.

To investigate the CM relation with respect to the dimensionless gate voltages N_1 and N_2, we start from the general expression for the electrical conductance $G[\Gamma_1(N_1), \Gamma_2(N_2)]$ derived in Ref. [22] [Appendix Eq. (A3)]. We now apply the CM relation in Eq. (1) to the 2SCKC. As shown in Fig. 1(b), the energy variable entering Eq. (1) is identified with the gate voltage V_g. The corresponding derivative can be expressed as

$$\frac{\partial}{\partial V_g} = \frac{C_{g1}\mathcal{R}_1}{e}\frac{\partial}{\partial N_1} + \frac{C_{g2}\mathcal{R}_2}{e}\frac{\partial}{\partial N_2} = \frac{e}{2E_{C,1}}\frac{\partial}{\partial N_1} + \frac{e}{2E_{C,2}}\frac{\partial}{\partial N_2},$$

where $\mathcal{R}_1 = (R_2 + R_3)/R_t$, $\mathcal{R}_2 = R_3/R_t$ are the resistance ratios of the voltage divider. These ratios depend solely on the external circuit and are independent of the 2SCKC. Consequently, the CM relation in Eq. (1) for the 2SCKC takes the form (in the units $\hbar = c = k_B = 1$)

$$S_{\rm CM} = \frac{\pi^2}{6e}\sum_{j=1,2}\mathcal{R}_j\frac{T}{E_{C,j}}\frac{\partial \ln G}{\partial N_j} = \frac{\pi^2}{6e}\sum_{j=1,2}\frac{T}{E_{C,j}}\frac{\partial \ln G}{\partial N_j}. \tag{3}$$

Without loss of generality, we choose $R_1 = R_2 = 0$ so that $\mathcal{R}_1 = \mathcal{R}_2 = 1$. This leads to the second equality.

The thermoelectric coefficients in the 2SCKC within the linear-response regime—where $[\Delta T, eV_{th}] \ll T$—have been computed and discussed in detail in Refs. [22,23,28]. The general expressions are presented in Appendix.

For the single-site charge Kondo circuit [9,15,20], it is mentioned that the conventional CM relation holds in the FL regime, where the temperature is much lower than the Kondo resonance width [$T \ll \Gamma$, where $\Gamma(N) = 8\gamma E_C|r|^2\cos^2(\pi N)/\pi^2$, $\gamma = e^{\mathbf{C}} \approx 1.78$ ($\mathbf{C} \approx 0.577$ is Euler's constant)] [9,19,20]. However, this relation breaks down in the NFL regime, in which $\Gamma \leqslant T \ll E_C$. To address this, we propose a GCM relation that remains valid in both FL and NFL regimes, covering the entire temperature range $T \ll E_C$.

III. GENERALIZED CUTLER-MOTT FORMULA

To analyze the CM relation, it is first necessary to examine the electrical conductance G [Appendix Eq. (A3)], where the function $F_C(\Gamma_1/T, \Gamma_2/T)$ is defined in Eq. (A4). Substituting Eq. (A3) into Eq. (3) yields the TP based on the CM relation,

$$S_{\rm CM} = \frac{4\gamma}{3e}\sum_{j=1,2}\frac{1}{F_C}\frac{\partial F_C}{\partial p_j}|r_j|^2\sin(2\pi N_j), \tag{4}$$

where $p_1 = \Gamma_1/T$, $p_2 = \Gamma_2/T$, $\Gamma_j = \Gamma(|r_j|, N_j)$, and

$$\frac{\partial F_C}{\partial p_1} = \int_{-\infty}^{\infty}dz\int_{-\infty}^{\infty}du\frac{p_2 u[u^2+4\pi^2]}{\sinh\left(\frac{u}{2}\right)\left[\cosh(z)+\cosh\left(\frac{u}{2}\right)\right]} \times \frac{\left[\left(z+\frac{u}{2}\right)^2 - p_1^2\right]}{\left[\left(z+\frac{u}{2}\right)^2+p_1^2\right]^2\left[\left(z-\frac{u}{2}\right)^2+p_2^2\right]}, \tag{5}$$

with an analogous expression for $\partial F_C/\partial p_2$.

As shown in Ref. [22], asymptotic expressions for the TP can be derived in four regimes: $(\Gamma_1,\ \Gamma_2) \ll T$, $\Gamma_1 \ll T \ll \Gamma_2$, $\Gamma_2 \ll T \ll \Gamma_1$, and $T \ll (\Gamma_1,\ \Gamma_2)$. In contrast, obtaining such asymptotic forms for $S_{\rm CM}$ directly from Eq. (5) is technically prohibitive. To overcome this difficulty, Kiselev introduced an analytical method for computing the scaling functions, which ensures their differentiability with respect to the relevant parameters [29]. This approach allows us, unlike Refs. [9,15,20], to express $F_C(\Gamma_1/T, \Gamma_2/T)$ in closed analytical forms.

In the regime $p_1 \ll 1$, $p_2 \ll 1$, the result is

$$F_C(p_1 \ll 1, p_2 \ll 1) = 4\pi^4 - \frac{\pi^3}{2}[16\ln(2) - 1](p_1 + p_2). \tag{6}$$

For $p_1 \gg 1$ or $p_2 \gg 1$, we obtain

$$\begin{aligned} F_C(p_1, p_2 \gg 1) &= \frac{1}{4p_2}\mathcal{P}(p_1), \\ F_C(p_1 \gg 1, p_2) &= \frac{1}{4p_1}\mathcal{P}(p_2), \\ \mathcal{P}(p) &= -4p^3 + \frac{2}{\pi}(p^4 - 10\pi^2 p^2 + 9\pi^4)\Psi^{(1)} \\ &\quad \times \left(\frac{1}{2} + \frac{p}{2\pi}\right) + \frac{124\pi^2 x}{3}, \end{aligned} \tag{7}$$

where $\Psi^{(1)}(x) = \sum_{n=0}^{\infty}(n+x)^{-2}$ is a tri-gamma function. Therefore, in the opposite limit, $p_1 \gg 1$, $p_2 \gg 1$, this yields

$$F_C(p_1 \gg 1, p_2 \gg 1) = \frac{64\pi^4}{5p_1p_2}. \tag{8}$$

Furthermore, in the limiting cases $p_1 = 0$ or $p_2 = 0$, corresponding to $\Gamma_1 = 0$ or $\Gamma_2 = 0$, exact analytical expressions are available,

$$\begin{aligned} F_C(0, p_2) &= \pi F_{C,0}(p_2), \\ F_C(p_1, 0) &= \pi F_{C,0}(p_1), \\ F_{C,0}(p) &= \pi(4\pi^2 - p^2)\left[1 - \frac{2p}{\pi}\Phi\left(-1, 1, 1 + \frac{p}{\pi}\right)\right] \\ &\quad + \frac{\pi^2 p}{2}, \end{aligned} \tag{9}$$

where $\Phi(r, s, z) = \sum_{n=0}^{\infty} r^n(n+z)^{-s}$ is the Lerch zeta function. These expressions are particularly useful for analyzing the system when one of the gate voltages is inactive, such as at $N_1 = 0$ or $N_2 = 0$, where the corresponding resonance width Γ_j vanishes.

Altogether, this analytical framework provides access to $\partial F_C/\partial p_j$, enabling a systematic investigation of the CM relation.

Comparing Eq. (4) with the general formula for TP obtained in Ref. [22] [rewritten in Eq. (A9)], we observe that the terms $\ln[E_{C,j}/(T + \Gamma_j)]$ are absent in the TP expression derived from the CM relation. This omission indicates that the traditional CM relation does not capture essential interaction effects.

As highlighted in Ref. [9], in the low-temperature regime ($T \ll \Gamma$), the system adheres to the FL paradigm. In this regime, TP S can be expressed in terms of the logarithmic derivative of conductance with respect to gate voltage, reflecting the sensitivity of the transport to electrostatic tuning. That form resembles the CM formula. However, the prefactor in this relation is significantly modified. In particular, it acquires an additional large factor $\ln(E_C/\Gamma)$, which encapsulates the influence of interaction-driven energy scales. In the high-temperature regime ($T \gg \Gamma$), the system crosses over to an NFL state, where the simple logarithmic derivative form of TP breaks down and there is no direct analog to the CM formula.

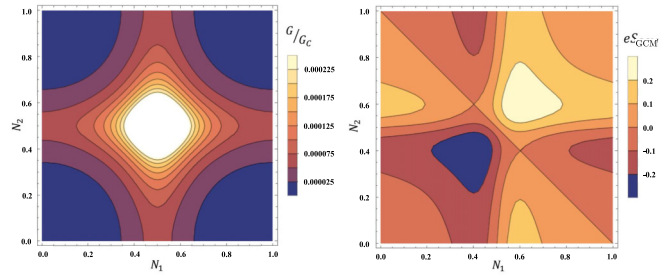

FIG. 2. Contour plots of electric conductance G/G_C and thermopower eS_{GCM} computed from Eq. (10) by applying GCM relation as functions of the dimensionless gate voltages N_1 and N_2 at temperature $T/E_C = 0.01$. In both contour graphs, $|r_1|^2 = |r_2|^2 = 0.1$ and $E_{C,1} = E_{C,2} = E_C$.

These observations motivate the development of a GCM relation that incorporates interaction effects and remains valid across both FL and NFL regimes. Building on Eq. (4), we therefore propose an expression for the thermoelectric response in the 2SCKC as

$$S_{\mathrm{GCM}} = \frac{4\gamma}{3e}\sum_{j=1,2}\frac{1}{F_C}\frac{\partial F_C}{\partial p_j}\ln\left[\frac{E_{C,j}}{T + \Gamma_j}\right]|r_j|^2\sin(2\pi N_j). \tag{10}$$

Equation (10) can be equivalently expressed in terms of the conductance derivative as

$$S_{\mathrm{GCM}} = \frac{\pi^2}{6e}\sum_{j=1,2}\frac{T}{E_{C,j}}\ln\left[\frac{E_{C,j}}{T + \Gamma_j}\right]\frac{\partial \ln G}{\partial N_j}. \tag{11}$$

Equations (10) and (11) represent the central results of this paper. We validate this GCM relation by examining its dependence on gate voltages, as shown in Fig. 2. While the electrical conductance is symmetric with respect to both N_1 and N_2, reaching its maximum at $N_1 = N_2 = 0.5$, the TP is symmetric along the line $N_2 = 1 - N_1$, where it vanishes and changes sign. Remarkably, the contour plot of TP calculated using Eq. (10) as a function of N_1 and N_2 exhibits the same qualitative features as the TP obtained directly from $S = G_T/G$, which is shown in Fig. 3 of Ref. [22].

We now examine the behavior of Eq. (10) in different limiting regimes, defined by the relative magnitudes of the energy scales (Γ_1, Γ_2, T).

A. (Γ_1, Γ_2) $\ll T$, non-Fermi liquid regime

In the limit where both resonance widths are much smaller than the temperature, i.e., (Γ_1, Γ_2) $\ll T$, the system enters the NFL regime. In this regime, the TP derived from the GCM formula, to leading (zeroth) order in Γ_1/T, Γ_2/T, is given by

$$S_{\mathrm{GCM}} = -\frac{\mathcal{C}_{\mathrm{CM},1}}{e}\sum_{j=1,2}|r_j|^2\ln\left(\frac{E_{C,j}}{T}\right)\sin(2\pi N_j), \tag{12}$$

where $\mathcal{C}_{\mathrm{CM},1} = 4(16\ln 2 - 1)\gamma/3(8\pi - 16\ln 2 + 1) \approx 1.593$. In comparison, the TP directly calculated in Ref. [22] exhibits weak NFL behavior at "high" temperature $T \gg (\Gamma_1, \Gamma_2)$,

and is given by

$$S = -\frac{\mathcal{C}_{\mathrm{dir},1}}{e}\sum_{j=1,2}|r_j|^2\ln\left(\frac{E_{C,j}}{T}\right)\sin(2\pi N_j), \tag{13}$$

where $\mathcal{C}_{\mathrm{dir},1} = 9\gamma/8 \approx 2$.

In terms of temperature scaling, Eq. (12) is consistent with both the perturbative result and the direct calculation in Eq. (13). The proximity of the prefactors $\mathcal{C}_{\mathrm{CM},1}$ and $\mathcal{C}_{\mathrm{dir},1}$, suggests that the GCM relation remains valid in the NFL regime.

B. $\Gamma_1 \ll T \ll \Gamma_2$, non-Fermi liquid on the left and Fermi liquid on the right CKC

This regime arises when the gate voltage N_1 is tuned closer to a Coulomb peak than N_2, so that the left QD exhibits NFL behavior, while the right dot remains in the FL regime. The TPs obtained from the two approaches—the GCM relation and direct calculation—are given below:

$$S_{\mathrm{GCM}} = -\frac{\mathcal{C}_{\mathrm{CM},2}}{e}|r_1|^2\ln\left(\frac{E_{C,1}}{T}\right)\sin(2\pi N_1) - \frac{\pi^2}{3e}\frac{T}{E_{C,2}}\ln\left(\frac{\pi^2}{8\gamma|r_2|^2\cos^2(\pi N_2)}\right)\tan(\pi N_2), \tag{14}$$

with $\mathcal{C}_{\mathrm{CM},2} = 8\gamma[189\zeta(3) - 68]/81\pi^3 \approx 0.903114$, where $\zeta(3) \approx 1.20206$ is the Riemann zeta function, which is related to the tetragamma function via $\Psi^{(2)}(1/2) = -14\zeta(3)$,

$$S = -\frac{\mathcal{C}_{\mathrm{dir},2}}{e}|r_1|^2\ln\left(\frac{E_{C,1}}{T}\right)\sin(2\pi N_1) - \frac{\pi^3}{3e}\frac{T}{E_{C,2}}\ln\left(\frac{\pi^2}{8\gamma|r_2|^2\cos^2(\pi N_2)}\right)\tan(\pi N_2), \tag{15}$$

where $\mathcal{C}_{\mathrm{dir},2} = 1024\gamma/75\pi^2 \approx 2.46$.

We find that the TPs in both Eqs. (14) and (15) consist of two distinct contributions: one reflecting the FL behavior of the right CKC, and the other capturing the NFL characteristics of the left subsystem. From Eq. (14), it is apparent that the original CM law applies well to the FL component but fails to accurately describe the NFL part. However, there exists an intermediate temperature regime, $T^* \ll T \ll \Gamma_2$ (where T^* determined in Eq. (45) of Ref. [22]), where the original CM relation remains valid. In contrast, by comparing Eqs. (14) and (15), it is clear that the GCM formula provides an accurate description for both components of the system, regardless of whether the underlying physics is FL or NFL.

C. $\Gamma_2 \ll T \ll \Gamma_1$, Fermi liquid on the left and non-Fermi liquid on the right CKC

This case is the converse of case in the above subsection, occurring when the gate voltage N_2 is tuned closer to the Coulomb peak than N_1. In this regime, the GCM formula yields the TP in the following form:

$$S_{\mathrm{GCM}} = -\frac{\pi^2}{3e}\frac{T}{E_{C,1}}\ln\left(\frac{\pi^2}{8\gamma|r_1|^2\cos^2(\pi N_1)}\right)\tan(\pi N_1) - \frac{\mathcal{C}_{\mathrm{CM},2}}{e}\ln\left(\frac{E_{C,2}}{T}\right)|r_2|^2\sin(2\pi N_2). \tag{16}$$

The TP directly computed for this case also comprises two components: a FL characteristic on the left circuit and a NFL property on the right,

$$S = -\frac{\pi^3}{3e}\frac{T}{E_{C,1}}\ln\left(\frac{E_{C,1}}{\Gamma_1}\right)\tan(\pi N_1) - \frac{\mathcal{C}_{\mathrm{dir},2}}{e}|r_2|^2\ln\left(\frac{E_{C,2}}{T}\right)\sin(2\pi N_2). \tag{17}$$

In this limit, the GCM relation remains applicable to both parts of the system. In contrast, the original CM relation fails to describe the right part, which exhibits NFL behavior, but still accurately captures the FL characteristics of the left part. Notably, the CM relation holds within the temperature window $T^{**} \ll T \ll \Gamma_1$, where T^{**} is defined in Eq. (47) of Ref. [22].

D. $T \ll (\Gamma_1, \Gamma_2)$, Fermi-liquid regime

This limit corresponds to the infinitesimally low temperature regime, which is inaccessible to perturbative approaches. The TPs obtained from both methods exhibit a linear temperature dependence and can be expressed analytically as

$$S_{\mathrm{GCM}} = -\frac{\pi^2}{3e}\sum_{j=1,2}\frac{T}{E_{C,j}}\ln\left[\frac{\pi^2}{8\gamma|r_j|^2\cos^2(\pi N_j)}\right]\tan(\pi N_j), \tag{18}$$

and

$$S = -\frac{3\pi^3}{7e}\sum_{j=1,2}\frac{T}{E_{C,j}}\ln\left[\frac{\pi^2}{8\gamma|r_j|^2\cos^2(\pi N_j)}\right]\tan(\pi N_j). \tag{19}$$

Similarly to the regimes discussed above, the close agreement between Eqs. (18) and (19) confirms the validity of the GCM theory in the full-FL regime. Our proposed GCM formula [Eq. (10)] not only remains consistent with Eq. (4) in Ref. [9], but also provides deeper insight into the thermoelectric response of strongly correlated nanostructures.

The results of the four different regimes demonstrate that the GCM formula serves as a standard benchmark for the 2SCKC, regardless of whether the system is in the FL or NFL state [9,15,19,21]. Furthermore, the application of the GCM formula across these four regimes reinforces our confidence in the advantages of a nonperturbative approach to the two-channel charge Kondo problem.

We now examine Eq. (10) numerically. The comparison reveals a strong consistency between the GCM formula and the direct calculation, which differs only by a constant prefactor of approximately 2.22. This agreement is illustrated in Fig. 3, where the blue curves—generated using the GCM relation [Eq. (10)]—closely follow the behavior of the black curves, which are obtained from direct evaluations of Eq. (A9). The presence of the logarithmic term in the GCM expression effectively captures the hallmark features of Kondo correlations and reinforces the interpretation of NFL behavior.

A notable feature of both the numerical results and the analytical limits considered in Secs. III A–III D is that the GCM expressions differ from the direct calculations only by

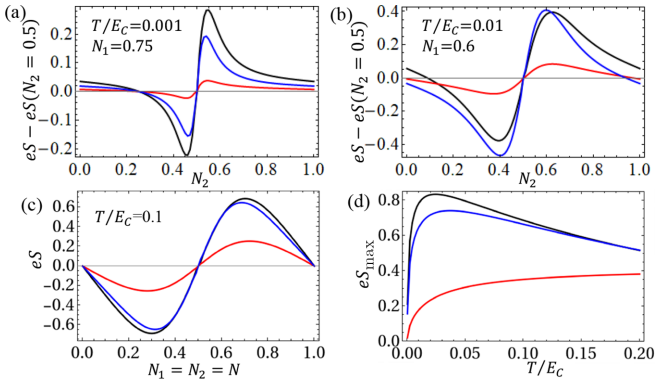

FIG. 3. Thermopower eS as a function of the gate voltage N_2 at different temperatures. (a) $T/E_C = 0.001$, $N_1 = 0.75$, (b) $T/E_C = 0.01$, $N_1 = 0.6$, and (c) $T/E_C = 0.1$, $N_1 = N_2 = N$. Panel (d) shows the maximum of thermopower as a function of temperature T/E_C. In all graphs, $|r_1|^2 = |r_2|^2 = 0.1$. The black lines are directly plotted (as in Ref. [22]), the red lines are plotted from the original Cutler-Mott formula [see Eq. (3)] multiplied by a factor of 2.22, and the blue lines are plotted from the generalized Cutler-Mott relation [see Eq. (10)], also multiplied by the same factor to match the red line in each panel.

overall prefactors of order unity. These adjustable factors are likely related to the inherent ambiguity in defining the Kondo temperature, $T_K \sim E_C$. In Eq. (1), the derivative is evaluated at $E = E_F$; however, in the strong- and intermediate-coupling regimes the role of the Fermi energy E_F is effectively played by the Kondo scale T_K. As is well known, T_K is a crossover scale separating the weak-coupling regime ($T \gg T_K$) from the intermediate/strong-coupling regimes ($T \ll T_K$) in the 1CK model.

For the 2CK model [30], the Kondo temperature T_K defined in the weak-coupling regime ($T \gg T_K$) does not coincide exactly with the scale extracted from the intermediate or strong-coupling regime ($T \ll T_K$). An analogous behavior arises in our system, where the characteristic scales inferred from the weak-coupling regime ($T \gg \Gamma_j$) and from the intermediate/strong-coupling regime ($T \ll \Gamma_j$) differ by a multiplicative factor of order unity.

Moreover, different physically motivated definitions of T_K—based on thermodynamic quantities (free energy, susceptibility, etc.) or transport observables (conductance, etc.)—lead to slightly different numerical estimates of the Kondo scale [30–32]. As a result, when the GCM relation is expressed in terms of these scales, the corresponding prefactors that appear in the NFL regimes naturally differ by order-one numerical factors.

IV. APPLICATION OF THE GENERALIZED CUTLER-MOTT RELATION TO SOME CHARGE KONDO SETUPS

In this section, we apply the GCM relation to two distinct charge Kondo implementations that are related to the 2SCKC. These setups provide practical platforms to test and illustrate the relevance of the GCM framework in experimentally motivated configurations.

A. Effect of one gate voltage is inactive: Either $N_1 = 0.5$ or $N_2 = 0.5$

In the limit $N_1 = 0.5$, $N_2 = N$, the TP is calculated from GCM as shown in Eq. (10) is

$$S_{\rm GCM} = \frac{4\gamma}{3e}\frac{\partial_p F_{C,0}(p)}{F_{C,0}(p)}|r|^2 \ln\left[\frac{E_C}{T+\Gamma}\right]\sin(2\pi N), \tag{20}$$

with $p = \Gamma/T$ and $F_{C,0}(p)$ is defined in Eq. (9). The TP as a function of gate voltage in this limit can be seen in the right panel of Fig. 2. At exact Coulomb peaks (i.e., when either $N_1 = 0.5$ or $N_2 = 0.5$), the particle-hole symmetry is preserved, irrespective of the scattering at the QPCs. As a result, the contribution from the corresponding segment of the system to the TP vanishes.

Interestingly, either $N_1 = 0.5$ or $N_2 = 0.5$ situation reduces to the case similar to the Matveev-Andreev (MA) setup [15], in which the left (right) structure simply is a normal metal lead, the electrical conductance in Eq. (A3) becomes $G = (G_C T/8\gamma E_C)\int dx(x^2+\pi^2)/[\cosh^2(x/2)\{x^2+(\Gamma/T)^2\}]$ and the Eq. (10) induces

$$S_{\rm GCM} = \frac{4\gamma}{3e}\ln\left[\frac{E_C}{T+\Gamma}\right]\frac{\partial_p F_0(p)}{F_0(p)}|r|^2\sin(2\pi N), \tag{21}$$

with [29]

$$F_0(p) = \int_{-\infty}^{\infty} dx \frac{x^2+\pi^2}{\cosh^2(x/2)}\frac{p}{x^2+p^2} = 2\pi\Psi^{(1)}\left(\frac{1}{2}+\frac{p}{2\pi}\right) + 4p\left[1-\frac{p}{2\pi}\Psi^{(1)}\left(\frac{1}{2}+\frac{p}{2\pi}\right)\right]. \tag{22}$$

So

$$\partial_p F_0(p) = 4 - \frac{4p}{\pi}\Psi^{(1)}\left(\frac{1}{2}+\frac{p}{2\pi}\right) + \left[1-\frac{p^2}{\pi^2}\right]\Psi^{(2)}\left(\frac{1}{2}+\frac{p}{2\pi}\right). \tag{23}$$

Replacing Eqs. (22) and (23) in Eq. (21), we obtain the generalized formula of Eq. (32) in Ref. [20] with added prefactor $\ln[E_C/(T+\Gamma)]$.

In the limit $T \ll \Gamma$, we obtain

$$S_{\rm GCM} = -\frac{\pi^2}{3e}\ln\left[\frac{E_C}{\Gamma}\right]\frac{T}{E_C}\tan(\pi N). \tag{24}$$

The result is in agreement with that reported in Ref. [9], except for a discrepancy in the prefactor, which is $-5/3\pi$. Remarkably, the coefficient presented in Eq. (4) of Ref. [9] deviates from that in the original CM relation.

In the opposite limit $T \gg \Gamma$, from Eq. (21), we obtain the TP for single-site charge Kondo as

$$S_{\rm GCM} = \frac{8\gamma[2-7\zeta(3)]}{3\pi^3 e}\ln\left[\frac{E_C}{T}\right]|r|^2\sin(2\pi N). \tag{25}$$

Indeed, Eq. (25) is similar to Eq. (51) in Ref. [15] except for the constant prefactor. It covers the perturbative result. A general situation is shown in Fig. 4. We find that the GCM formula multiple of a factor 1.35 is stunningly consistent with the result of the direct calculation in Refs. [9,15].

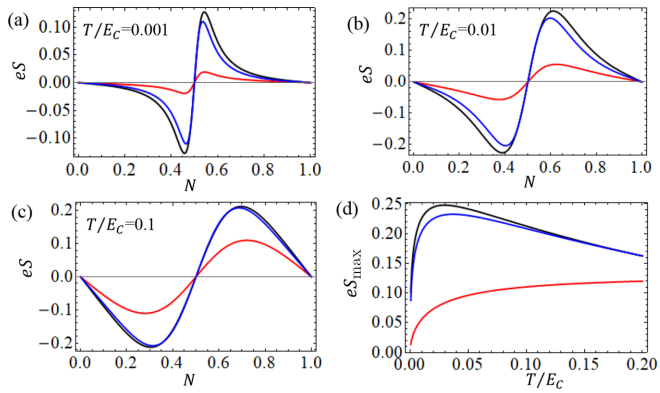

FIG. 4. Thermopower eS as a function of the gate voltage N at different temperatures. (a) $T/E_C = 0.001$, (b) $T/E_C = 0.01$, and (c) $T/E_C = 0.1$. Panel (d) shows the maximum of thermopower as a function of temperature T/E_C. In all graphs, $|r|^2 = 0.1$. The black lines are plotted directly (as in Refs. [9,15]), the red lines are plotted from the original Cutler-Mott formula [see Eq. (3)], multiplied by a factor of 1.35, and the blue lines are plotted from the generalized Cutler-Mott relation [see Eq. (21)], also multiplied by a factor of 1.35.

B. Strongly asymmetric reflection amplitudes $|r_1|^2 \ll |r_2|^2$ in the weak coupling between single- and two-channel charge Kondo circuits

The description of the weakly coupled single- and two-channel Kondo simulators involves the left CKC being in the FL-1CK state and the right CKC operating in the NFL-2CK state. According to Ref. [22], when $|r_1|^2 \ll |r_2|^2$, the TP is

$$S = -\frac{12\gamma}{5\pi e}\frac{F_T(p_2)}{F_G(p_2)}|r_2|^2 \ln\left(\frac{E_{C,2}}{T+\Gamma_2}\right)\sin(2\pi N_2), \tag{26}$$

with [29]

$$F_G(p_2) = \int_{-\infty}^{\infty} du \frac{p_2(u^2+\pi^2)(u^2+9\pi^2)}{\cosh^2\left(\frac{u}{2}\right)\left(u^2+p_2^2\right)} = -4p_2^3 + \frac{124\pi^2}{3}p_2 + \frac{2}{\pi}\left(p_2^4 - 10\pi^2 p_2^2 + 9\pi^4\right)\Psi^{(1)} \times \left(\frac{1}{2}+\frac{p_2}{2\pi}\right), \tag{27}$$

and [29]

$$F_T(p_2) = \int_{-\infty}^{\infty} du \frac{u^2(u^2+\pi^2)(u^2+9\pi^2)}{\cosh^2\left(\frac{u}{2}\right)\left(u^2+p_2^2\right)} = 4p_2^4 - \frac{124\pi^2}{3}p_2^2 + \frac{256\pi^4}{5} - \frac{2}{\pi}\left(p_2^5 - 10\pi^2 p_2^3 + 9\pi^4\right)\Psi^{(1)}\left(\frac{1}{2}+\frac{p_2}{2\pi}\right), \tag{28}$$

The TP obtained from GCM formula [Eq. (10)] has the form

$$S_{\rm GCM} = \frac{4\gamma}{3e}\frac{\partial_{p_2}F_G}{F_G}\ln\left(\frac{E_{C,2}}{T+\Gamma_2}\right)|r_2|^2\sin(2\pi N_2). \tag{29}$$

We demonstrate the consistency of the GCM formula with the direct calculation in Fig. 5.

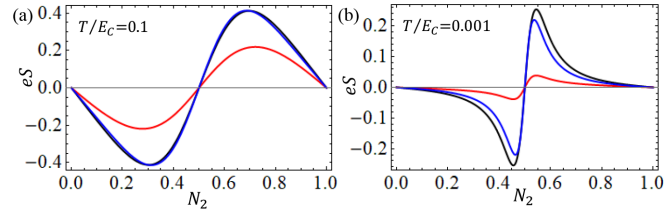

FIG. 5. Thermopower eS as a function of the gate voltage N_2 at different temperatures. (a) $T/E_C = 0.1$ and (b) $T/E_C = 0.001$. In both graphs, $|r_2|^2 = 0.1$. The black lines are plotted directly [see Eq. (26)], the red lines are plotted from the original Cutler-Mott formula, multiplied by a factor of 2.8, and the blue lines are plotted from the generalized Cutler-Mott relation [see Eq. (29)], also multiplied by the same factor of 2.8.

V. GENERALIZED CUTLER-MOTT RELATION FOR THE FIGURE OF MERIT ZT

The figure of merit, denoted as ZT, is a critical parameter in evaluating the performance of thermoelectric materials. It combines the material's thermoelectric efficiency by incorporating its electric conductance G, thermal conductance $\mathcal{K}$, and TP S into a single dimensionless quantity. The figure of merit is defined as [4]

$$ZT = \frac{S^2GT}{\mathcal{K}}; \quad \mathcal{K} = \left.\frac{\partial I_h}{\partial \Delta T}\right|_{I_e=0} = G_H - T\frac{G_T^2}{G}. \tag{30}$$

A high ZT indicates a material's potential for efficient thermoelectric conversion, with high values of ZT leading to better performance in applications such as power generation and cooling. The goal in thermoelectric research is to maximize ZT, which requires optimizing the balance between electrical and thermal conductivity. While high electrical conductance is desirable for efficient charge transport, low thermal conductance is equally important to prevent the loss of heat. Achieving high thermoelectric efficiency is thus a complex challenge that requires careful material design, particularly in advanced materials with low-dimensional or nanostructured properties. As such, the figure of merit plays a pivotal role in guiding the development of next-generation thermoelectric materials that could significantly improve energy conversion efficiency in practical devices.

Interestingly, the ratio of the electronic thermal conductance $\mathcal{K}$ and the electrical conductance G is stated in the WF law. It is known that in the low-temperature regime of a macroscopic sample, this ratio is proportional to the temperature T, with the proportionality constant being the Lorenz number L_0 [33,34],

$$\frac{\mathcal{K}}{G} = L_0 T, \tag{31}$$

where $L_0 = \pi^2/3$. Although transport in nanodevices is generally expected to deviate from the WF law, even within the FL regime [33], recent reports suggest that the WF law holds even in the NFL regime of Kondo effects [35,36]. Moreover, the universal value of the Lorenz ratio $R \equiv L/L_0 = (3/\pi^2)(\mathcal{K}/GT)$ exhibits charge Kondo correlations [20]. For

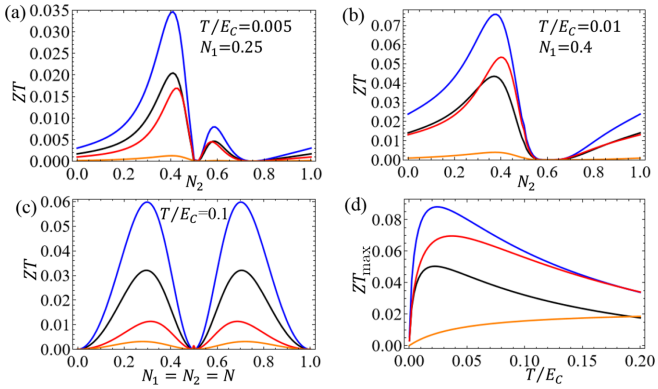

FIG. 6. Figure of merit ZT as a function of the gate voltage N_2 at different temperatures. (a) $T/E_C = 0.005$, $N_1 = 0.25$, (b) $T/E_C = 0.01$, $N_1 = 0.4$, and (c) $T/E_C = 0.1$, $N_1 = N_2 = N$. Panel (d) shows the maximum of figure of merit $ZT_{\max}$ as a function of temperature T/E_C. In all graphs, $|r_1|^2 = |r_2|^2 = 0.1$. The black lines are directly plotted [as in Eq. (30)], the blue lines are plotted by approximated computation [as in Eq. (33)], the orange lines are plotted from the original CM formula multiplied by a factor of 4.93, and the red lines are plotted from the GCM relation [see Eqs. (34) and (35)], also multiplied by the same factor to match the orange line in each panel.

the 2SCKC, the Lorenz ratio satisfies [37]

$$R = \frac{12}{5} - \frac{3}{\pi^2}S^2. \tag{32}$$

As we find in the previous sections, $S \ll 1$, we can have

$$ZT \approx \frac{5}{4\pi^2}S^2. \tag{33}$$

Therefore, we can get the GCM relation for the figure of merit as

$$ZT_{\rm GCM} = \frac{5\pi^2}{144e^2}\left[\sum_{j=1,2}\frac{T}{E_{C,j}}\ln\left(\frac{E_{C,j}}{T+\Gamma_j}\right)\frac{\partial \ln G}{\partial N_j}\right]^2, \tag{34}$$

or

$$ZT_{\rm GCM} \approx \frac{20\gamma^2}{9e^2\pi^2}\left[\sum_{j=1,2}\frac{1}{F_C}\frac{\partial F_C}{\partial p_j}\ln\left(\frac{E_{C,j}}{T+\Gamma_j}\right)|r_j|^2\sin(2\pi N_j)\right]^2. \tag{35}$$

The GCM relation for figure of merit in Eq. (35) is now examined numerically. In Fig. 6, we show the plots of figure of merit obtained from direct calculation in Eq. (30) [black lines, with G, G_T, G_H are taken from general formulas (A3), (A6), and (A10)], approximated computation in Eq. (33) (blue lines), CM relation multiplied by a factor of 4.93 (orange lines), and GCM relation in Eqs. (34) and (35) (red lines). The most important plot is the maximum value of ZT as a function of temperature T/E_C [see Fig. 6(d)], which demonstrates the consistency between the GCM formula and the direct calculation; the two (red and blue) curves differ only by an overall factor of 4.93, originating from the differential factor 2.22 in the TP. Notably, the red lines exhibit the same behavior as the black and blue lines [obtained from direct calculations in Eqs. (30) and (33)]. The logarithmic term in the GCM expression captures the essence of Kondo correlations and supports the NFL interpretation.

VI. CONCLUSIONS

In summary, we have introduced GCM formula for quantum circuits with weak coupling between two QD-QPC structures, each realizing a charge Kondo simulator. Our proposal is motivated by a detailed comparison between the TP obtained from the traditional CM relation and the TP calculated nonperturbatively in Ref. [22].

The TP derived via the nonperturbative framework not only reproduces the perturbative limit but also remains valid deep into the low-temperature regime, $T \ll \min[|r_j|^2 E_{C,j}]$. While previous work [9,20] established that the CM formula accurately captures the FL regime ($T \ll \min[|r_j|^2 E_{C,j}]$) and deviates as the system enters the NFL regime ($T \gg \max[|r_j|^2 E_{C,j}]$), our GCM formulation remains applicable across the full temperature range. That is, at low temperatures ($T \ll \min[|r_j|^2 E_{C,j}]$), the GCM relation offers an FL diagnostic analogous to the CM formula, while at high temperatures ($T \gg \max[|r_j|^2 E_{C,j}]$), it captures emergent NFL behavior through the characteristic dependence $\ln[E_{C,j}/T]$ associated with strong isospin correlations. We further demonstrate that the GCM relation is robust in all charge Kondo configurations examined, including symmetric 2CK-2CK setups, strongly asymmetric 1CK-2CK hybrids, and one-site models.

Beyond TP, the GCM framework naturally extends to thermoelectric performance metrics such as the figure of merit ZT. The general recipe for constructing the GCM involves incorporating modification terms of the form $\{\ln[E_C/(T+\Gamma_j)]\}^2$ for each $\partial F_C/\partial\Gamma_j$, where j indexes the relevant Kondo resonance widths of the charge Kondo system. This prescription provides a systematic route to incorporating strong correlation effects into thermoelectric response functions.

The applicability of the GCM relation beyond the 2SCKC setup follows from the general structure of the underlying transport theory. Derived within linear response, the GCM relation does not rely on the existence of long-lived quasiparticles or on FL phenomenology. Instead, it reflects general connections between charge and heat current correlators and the energy dependence of interacting spectral functions governing transport. The models studied here constitute minimal, yet, experimentally relevant platforms in which strong correlations and nontrivial many-body effects coexist with the validity of the GCM relation across distinct regimes. This robustness indicates that the GCM captures universal features of thermoelectric response dictated by conservation laws, symmetries, and low-energy scaling, rather than model-specific details [38,39]. We therefore expect analogous GCM relations to hold in a broader class of strongly correlated systems, including other quantum impurity models and correlated mesoscopic conductors, provided transport is governed by similar linear-response mechanisms.

ACKNOWLEDGMENTS

This research in Hanoi is funded by Vietnam National Foundation for Science and Technology Development

(NAFOSTED) under Grant No. 103.01-2023.03. T.K.T.N. would like to acknowledge support from the ICTP through the Associates Programme (2024-2029). The work of M.N.K. is conducted within the framework of the Trieste Institute for Theoretical Quantum Technologies (TQT).

DATA AVAILABILITY

The data that support the findings of this article are not publicly available. The data are available from the authors upon reasonable request.

APPENDIX: PREVIOUS RESULTS

To study the thermoelectric effects at the weak link between two QDs in the linear-response regime, where $[\Delta T, eV_{th}] \ll T$, we build on the theoretical framework developed in Refs. [22,23,28]. This approach evaluates both the charge current I_e and heat current I_h through the tunnel contact based on the Onsager reciprocity relations [40].

Central to this analysis is the local density of states of the QDs at the weak link, which are expressed using the correlation function $K_j(1/2T + it)$. This function captures the effects of Coulomb interactions and is derived following the Matveev-Andreev theory [9,15]. Near the Coulomb blockade peaks, the Kondo-resonance width Γ_j plays a significant role, and is given by

$$\Gamma_j(N_j) = \frac{8\gamma E_{C,j}}{\pi^2}|r_j|^2\cos^2(\pi N_j). \tag{A1}$$

The leading-order expression for the correlation function is

$$\begin{aligned} K_j\left(\frac{1}{2T}+it\right) &= \frac{\pi T\Gamma_j}{\gamma E_{C,j}}\frac{1}{\cosh(\pi Tt)} \\ &\times \int_{-\infty}^{\infty}\frac{e^{\omega(1/2T+it)}}{(\omega^2+\Gamma_j^2)(1+e^{\omega/T})}d\omega \\ &- \frac{4T}{E_{C,j}}\frac{|r_j|^2\sin(2\pi N_j)}{\cosh(\pi Tt)}\ln\left(\frac{E_{C,j}}{T+\Gamma_j}\right) \\ &\times \int_{-\infty}^{\infty}\frac{\omega e^{\omega(1/2T+it)}}{(\omega^2+\Gamma_j^2)(1+e^{\omega/T})}d\omega. \end{aligned} \tag{A2}$$

Using these expressions, the transport coefficients [40] in the linear-response regime can be derived as follows [22,23,28] (in the units $\hbar = c = k_B = 1$).

The electric conductance $G = \partial I_e/\partial\Delta V|_{\Delta T=0}$ is obtained as

$$G = \frac{G_C}{24\gamma^2}\frac{T^2}{E_{C,1}E_{C,2}}F_C\left(\frac{\Gamma_1}{T},\frac{\Gamma_2}{T}\right), \tag{A3}$$

where $G_C = 2\pi e^2\nu_{0,1}\nu_{0,2}|t|^2$ is a conductance of the central (tunnel) area, which is characterized by the tunneling amplitude $|t|$, local densities of states $\nu_{0,1}$, $\nu_{0,2}$ assuming that the electrons in the QDs are noninteracting,

$$F_C(p_1,p_2) = \int_{-\infty}^{\infty}dz\int_{-\infty}^{\infty}du\,F(p_1,p_2,z,u), \tag{A4}$$

in which $p_1 = \Gamma_1/T$ and $p_2 = \Gamma_2/T$,

$$\begin{aligned} F(p_1,p_2,z,u) &= \frac{p_1p_2u[u^2+4\pi^2]}{\sinh\left(\frac{u}{2}\right)\left[\cosh(z)+\cosh\left(\frac{u}{2}\right)\right]} \\ &\times \frac{1}{\left[\left(z+\frac{u}{2}\right)^2+p_1^2\right]\left[\left(z-\frac{u}{2}\right)^2+p_2^2\right]}. \end{aligned} \tag{A5}$$

The thermoelectric coefficient $G_T = \partial I_e/\partial\Delta T|_{\Delta V=0}$ is

$$\begin{aligned} G_T = &-\frac{G_C}{6e\gamma\pi}\frac{T^3}{E_{C,1}E_{C,2}} \\ &\times\left\{\frac{|r_1|^2}{\Gamma_1}\ln\left(\frac{E_{C,1}}{T+\Gamma_1}\right)\sin(2\pi N_1)F_{T,s}\left(\frac{\Gamma_1}{T},\frac{\Gamma_2}{T}\right)\right. \\ &\left.\times\frac{|r_2|^2}{\Gamma_2}\ln\left(\frac{E_{C,2}}{T+\Gamma_2}\right)\sin(2\pi N_2)F_{T,m}\left(\frac{\Gamma_1}{T},\frac{\Gamma_2}{T}\right)\right\}, \end{aligned} \tag{A6}$$

where

$$F_{T,s}(p_1,p_2) = \int_{-\infty}^{\infty}dz\int_{-\infty}^{\infty}du\left(z+\frac{u}{2}\right)zF(p_1,p_2,z,u), \tag{A7}$$

$$F_{T,m}(p_1,p_2) = \int_{-\infty}^{\infty}dz\int_{-\infty}^{\infty}du\left(z-\frac{u}{2}\right)zF(p_1,p_2,z,u). \tag{A8}$$

Therefore, the TP can be written as

$$\begin{aligned} S = &-\frac{4\gamma}{e\pi}\frac{1}{F_C\left(\frac{\Gamma_1}{T},\frac{\Gamma_2}{T}\right)} \\ &\times\left\{|r_1|^2\frac{T}{\Gamma_1}\ln\left(\frac{E_{C,1}}{T+\Gamma_1}\right)\sin(2\pi N_1)F_{T,s}\left(\frac{\Gamma_1}{T},\frac{\Gamma_2}{T}\right)\right. \\ &\left.+|r_2|^2\frac{T}{\Gamma_2}\ln\left(\frac{E_{C,2}}{T+\Gamma_2}\right)\sin(2\pi N_2)F_{T,m}\left(\frac{\Gamma_1}{T},\frac{\Gamma_2}{T}\right)\right\}. \end{aligned} \tag{A9}$$

The thermal coefficient (or heat current response) $G_H = \partial I_h/\partial\Delta T|_{\Delta V=0}$ is obtained as

$$G_H = \frac{G_C}{240\gamma^2e^2}\frac{T^3}{E_{C,1}E_{C,2}}F_H\left(\frac{\Gamma_1}{T},\frac{\Gamma_2}{T}\right), \tag{A10}$$

where

$$\begin{aligned} F_H(p_1,p_2) = &\int_{-\infty}^{\infty}dz\int_{-\infty}^{\infty}du(-9u^2+20z^2+16\pi^2) \\ &\times F(p_1,p_2,z,u). \end{aligned} \tag{A11}$$

These analytical results form the basis for evaluating the transport properties in the current study, where we further explore the expressions for TP and the figure of merit from the CM and GCM formulas.

[1] C. Wood, Materials for thermoelectric energy conversion, Rep. Prog. Phys. **51**, 459 (1988).

[2] T. J. Seebeck, Über den Magnetismus der galvanischen Kette, Abh. Akad. Wiss. Berlin **1820-21**, 289 (1822); *Magnetische*

Polarisation der Metalle und Erze durch Temperatur-Differenz (W. Engelmann, Leipzig, 1825).

[3] D. K. C. MacDonald, *Thermoelectricity: An Introduction to the Principles* (Wiley, New York, 1962).

[4] H. J. Goldsmid, *Introduction to Thermoelectricity* (Springer-Verlag, Berlin, 2009).

[5] D. Boese and R. Fazio, Thermoelectric effects in Kondo-correlated quantum dots, Europhys. Lett. **56**, 576 (2001); B. Dong and X. L. Lei, Effect of the Kondo correlation on the thermopower in a quantum dot, J. Phys.: Condens. Matter **14**, 11747 (2002); M. Krawiec and K. I. Wysokiński, Thermoelectric effects in strongly interacting quantum dot coupled to ferromagnetic leads, Phys. Rev. B **73**, 075307 (2006); T. A. Costi, A. C. Hewson, and V. Zlatíc, Transport coefficients of the Anderson model via the numerical renormalization group, J. Phys.: Condens. Matter **6**, 2519 (1994).

[6] M. Cutler and N. F. Mott, Observation of Anderson localization in an electron gas, Phys. Rev. **181**, 1336 (1969).

[7] P. Dollfus, V. H. Nguyen, and J. Saint-Martin, Thermoelectric effects in graphene nanostructures, J. Phys.: Condens. Matter **27**, 133204 (2015).

[8] M. Turek and K. A. Matveev, Cotunneling thermopower of single electron transistors, Phys. Rev. B **65**, 115332 (2002).

[9] A. V. Andreev and K. A. Matveev, Coulomb blockade oscillations in the thermopower of open quantum dots, Phys. Rev. Lett. **86**, 280 (2001).

[10] R. Scheibner, H. Buhmann, D. Reuter, M. N. Kiselev, and L. W. Molenkamp, Thermopower of a Kondo spin-correlated quantum dot, Phys. Rev. Lett. **95**, 176602 (2005).

[11] A. Hewson, *The Kondo Problem to Heavy Fermions* (Cambridge University Press, Cambridge, 1993).

[12] K. Flensberg, Capacitance and conductance of mesoscopic systems connected by quantum point contacts, Phys. Rev. B **48**, 11156 (1993).

[13] K. A. Matveev, Coulomb blockade at almost perfect transmission, Phys. Rev. B **51**, 1743 (1995).

[14] A. Furusaki and K. A. Matveev, Coulomb blockade oscillations of conductance in the regime of strong tunneling, Phys. Rev. Lett. **75**, 709 (1995).

[15] K. A. Matveev and A. V. Andreev, Thermopower of a single-electron transistor in the regime of strong inelastic cotunneling, Phys. Rev. B **66**, 045301 (2002).

[16] K. Le Hur and G. Seelig, Capacitance of a quantum dot from the channel-anisotropic two-channel Kondo model, Phys. Rev. B **65**, 165338 (2002).

[17] Z. Iftikhar, S. Jezouin, A. Anthore, U. Gennser, F. D. Parmentier, A. Cavanna, and F. Pierre, Two-channel Kondo effect and renormalization flow with macroscopic quantum charge states, Nature (London) **526**, 233 (2015).

[18] Z. Iftikhar, A. Anthore, A. K. Mitchell, F. D. Parmentier, U. Gennser, A. Ouerghi, A. Cavanna, C. Mora, P. Simon, and F. Pierre, Tunable quantum criticality and super-ballistic transport in a "charge" Kondo circuit, Science **360**, 1315 (2018).

[19] T. K. T. Nguyen, M. N. Kiselev, and V. E. Kravtsov, Thermoelectric transport through a quantum dot: Effects of asymmetry in Kondo channels, Phys. Rev. B **82**, 113306 (2010).

[20] D. B. Karki, Coulomb blockade oscillations of heat conductance in the charge Kondo regime, Phys. Rev. B **102**, 245430 (2020).

[21] T. K. T. Nguyen and M. N. Kiselev, Protection of a non-Fermi liquid by spin-orbit interaction, Phys. Rev. B **92**, 045125 (2015).

[22] T. K. T. Nguyen, H. Q. Nguyen, and M. N. Kiselev, Thermoelectric transport across a tunnel contact between two charge Kondo circuits: Beyond perturbation theory, Phys. Rev. B **109**, 115139 (2024).

[23] T. K. T. Nguyen and M. N. Kiselev, Seebeck effect on a weak link between Fermi and non-Fermi liquids, Phys. Rev. B **97**, 085403 (2018).

[24] W. Pouse, L. Peeters, C. L. Hsueh, U. Gennser, A. Cavanna, M. A. Kastner, A. K. Mitchell, and D. Goldhaber-Gordon, Quantum simulation of an exotic quantum critical point in a two-site charge Kondo circuit, Nat. Phys. **19**, 492 (2023).

[25] Ph. Nozières and A. Blandin, Kondo effect in real metals, J. Phys. **41**, 193 (1980).

[26] A. M. Tsvelick and P. B. Wiegmann, Exact results in the theory of magnetic alloys, Adv. Phys. **32**, 453 (1983).

[27] N. Andrei, K. Furuya, and J. H. Lowenstein, Solution of the Kondo problem, Rev. Mod. Phys. **55**, 331 (1983).

[28] T. K. T. Nguyen and M. N. Kiselev, Heat conductance oscillations in two weakly connected charge Kondo circuits, Commun. Phys. **32**, 331 (2022).

[29] M. N. Kiselev, Universal scaling functions for a quantum transport through single-site and double-site charge Kondo circuits, Lecture notes in Physics (unpublished).

[30] N. Andrei and A. Jerez, Fermi- and non-Fermi-liquid behavior in the anisotropic multichannel Kondo model: Bethe Ansatz solution, Phys. Rev. Lett. **74**, 4507 (1995).

[31] N. Andrei and C. Destri, Solution of the multichannel Kondo problem, Phys. Rev. Lett. **52**, 364 (1984).

[32] G. Zaránd, T. Costi, A. Jerez, and N. Andrei, Thermodynamics of the anisotropic two-channel Kondo problem, Phys. Rev. B **65**, 134416 (2002).

[33] G. Benenti, G. Casati, K. Saito, and R. Whitney, Fundamental aspects of steady-state conversion of heat to work at the nanoscale, Phys. Rep. **694**, 1 (2017).

[34] V. Zlatíc and R. Monnier, *Modern Theory of Thermoelectricity* (Oxford University Press, Oxford, 2014).

[35] G. A. R. van Dalum, A. K. Mitchell, and L. Fritz, Wiedemann-Franz law in a non-Fermi liquid and Majorana central charge: Thermoelectric transport in a two-channel Kondo system, Phys. Rev. B **102**, 041111(R) (2020).

[36] D. B. Karki and M. N. Kiselev, Quantum thermoelectric and heat transport in the overscreened Kondo regime: Exact conformal field theory results, Phys. Rev. B **102**, 241402(R) (2020).

[37] M. N. Kiselev, Generalized Wiedemann-Franz law in a two site charge Kondo circuit: Lorenz ratio as a manifestation of the orthogonality catastrophe, Phys. Rev. B **108**, L081108 (2023).

[38] A. I. Pavlov and M. N. Kiselev, Universal relations between thermoelectrics and noise in mesoscopic transport across a tunnel junction, Phys. Rev. Lett. **136**, 046301 (2026).

[39] T. K. T. Nguyen, J. Rech, T. Martin, and M. N. Kiselev, Noises in a two-channel charge Kondo model, Phys. Rev. B **113**, 075430 (2026).

[40] L. Onsager, Reciprocal relations in irreversible processes. I., Phys. Rev. **37**, 405 (1931); Reciprocal relations in irreversible processes. II., **38**, 2265 (1931).